B. A. R. C.-1023

B. A. R. C.-1023

भारत सरकार
GOVERNMENT OF INDIA
परमाणु ऊर्जा आयोग
ATOMIC ENERGY COMMISSION

OCENER, A ONE-DIMENSIONAL COMPUTER CODE FOR THE NUMERICAL SIMULATION OF THE MECHANICAL EFFECTS OF PEACEFUL UNDERGROUND NUCLEAR EXPLOSIONS IN ROCKS

by

Satish C. Gupta, S. K. Sikka and R. Chidambaram
Neutron Physics Division

भाभा परमाणु अनुसंधान केन्द्र
BHABHA ATOMIC RESEARCH CENTRE
बंबई, भारत
BOMBAY, INDIA
1979

B. A. R. C. -1023

B. A. R. C. -1023

GOVERNMENT OF INDIA
ATOMIC ENERGY COMMISSION

OCENER, A ONE-DIMENSIONAL COMPUTER CODE FOR THE NUMERICAL SIMULATION OF THE MECHANICAL EFFECTS OF PEACEFUL UNDERGROUND NUCLEAR EXPLOSIONS IN ROCKS

by

Satish C. Gupta, S.K. Sikka and R. Chidambaram
Neutron Physics Division

BHABHA ATOMIC RESEARCH CENTRE
BOMBAY, INDIA
1979

INIS Subject Category : E14

Descriptors :

NUCLEAR EXPLOSIONS

UNDERGROUND EXPLOSIONS

CRATERING EXPLOSIONS

CONTAINED EXPLOSIONS

ROCKS

FRACTURES

CAVITIES

FINITE DIFFERENCE METHOD

ONE-DIMENSIONAL CALCULATIONS

SIMULATION

O CODES

OCENER, A ONE-DIMENSIONAL COMPUTER CODE FOR THE NUMERICAL SIMULATION OF THE MECHANICAL EFFECTS OF PEACEFUL UNDERGROUND NUCLEAR EXPLOSIONS IN ROCKS

by

Satish C. Gupta, S.K. Sikka and R. Chidambaram
Neutron Physics Division

ABSTRACT

An account is given of a one-dimensional spherical symmetric computer code for the numerical simulation of the effects of peaceful underground nuclear explosions in rocks (OCENER). In the code, the nature of the stress field and response of the medium to this field are modeled numerically by finite difference form of the laws of continuum mechanics and the constitutive relations of the rock medium in which the detonation occurs. It enables us to approximate well the cavity growth and fracturing of the surrounding rock for contained explosions and the events upto the time the spherical symmetry is valid for cratering-type explosions.

CONTENTS

		Page
I.	INTRODUCTION	1
II.	PHENOMENOLOGY OF UNDERGROUND NUCLEAR EXPLOSIONS	2
III.	BASIC EQUATIONS USED IN CODE	4
IV.	SOME COMPUTATIONAL DETAILS	6
	IV.1. SUBROUTINE EPFLOW	7
	IV.2. SUBROUTINE STATE	9
	IV.3. SUBROUTINE FAILURE	12
	IV.4. ARTIFICIAL VISCOSITY TERM	15
	IV.5. Δt CALCULATION	15
	IV.6. BOUNDARY CONDITIONS	16
	IV.7. INITIAL CONDITIONS	16
	IV.8. REZONING	17
	IV.9. SIMULATION OF OVERBURDEN PRESSURE	18
V.	SOME TYPICAL OUTPUTS	19
VI.	SAMPLE CALCULATIONS	20
	REFERENCES	22
	APPENDIX - INPUT INSTRUCTIONS	30

INTRODUCTION

For evaluating the economic feasibility of any application of peaceful underground nuclear explosions, it is essential that one be able to predict as accurately as possible the effects on the geological medium of such an explosion. Among other things, this entails being able to compute the nature of the stress field and the response of the medium to this field as a function of the explosion conditions. To date, a number of computer codes have been developed (Cherry and Petersen, 1970; Maury, 1970; Cameron and Scorgie, 1970) for these predictive purposes. These code models are based on the laws of continuum mechanics and constitutive relations of the rock medium in which detonation is carried out. To develop this predictive capability and also to explain the results of the 1974 Pokaran PNE experiment (Chidambaram and Ramanna, 1975), we started writing these codes. The purpose of this report is to document a one dimensional code for spherical symmetry (OCENER*). This can approximate well the phenomenology, i.e. cavity growth and fracture of the surrounding rock, for contained explosions. For cratering type of explosions, these calculations are valid upto the time the rarefaction wave from the surface meets the top of the growing cavity in the vertical direction. The code is similar to the American program 'SOC' and we have been heavily guided in

* One dimensional Code for Effects of Peaceful Underground Nuclear Explosions in Rocks.

writing this program by the papers of Cherry and Peterson (1970) and Schatz (1973, 1974). Before describing the method of calculation and the programing details, we give briefly the phenomenology of underground nuclear explosions and their effects on the rock medium so as to make clear what the code is expected to do.

II. PHENOMENOLOGY OF UNDERGROUND NUCLEAR EXPLOSIONS

The explosion of a nuclear device liberates 4.18×10^{19} ergs of energy per kiloton of yield in less than one microsecond. The device materials are brought to a temperature of several million degrees and a pressure of several megabars. Under such conditions, the device materials are vaporized. As this high pressure, high temperature gas pushes on the walls of the emplacement chamber, a strong shock wave propagates through the surrounding rock. This diverging shock wave loses its energy to the rock by distributing it as internal and kinetic energies and changes the state of the rock depending upon its mechanical properties and upon the energy deposited. Some of the changes are:

i) Vaporisation

The rock is vaporised immediately around the source. Butkovich (1967) has shown that, in silicate rocks, about 70 tons of rock are shock vaporised per kiloton of yield. About 20 per cent of the energy is lost in this process and is not available to

---

A nuclear kiloton = 1000 tons of TNT and energy content of 1g of TNT = 1000 calories.

participate in the mechanical effects of the explosions.

ii) Melting

About 300 tons/kt of rock is shock melted. The energy lost again is around 20 per cent.

iii) Crushing

In this process, any air pores (air-filled porosity) in the rock are removed.

iv) Rock Fracturing

This happens when the shear and tensile stresses created by initial and reflected stress waves exceed the respective failure stresses.

Meanwhile, as the shock wave is causing the above effects in the rock, the cavity containing the vaporised rock continues to expand spherically*. For deeply buried shots, this happens until the pressure of the vaporised rock mass inside the cavity and the stress field in the rock is the same. The spherical cavity so produced may remain stable or collapse, immediately or after some time, depending upon the type of the rock, the depth of burial and the explosive energy. Once this collapse initiates, it will progress upwards and terminate near the limit of the fractured zone, forming what is known as the chimney (see fig. 1).

For cratering type explosions, (depth of burial less than

---

* Rigorously true, if gravity effects are neglected.

$\sim$ 60 m multiplied by the cube root of the yield in kilotons) the first shock meets the ground surface and is reflected as a pressure-relieving rarefaction wave, which travels back towards the cavity. Tension developed due to this in the rock causes tensile fractures and may cause spallation of slabs of the rock material. When the rarefaction wave has met the growing cavity, the resulting pressure gradient between the cavity gas and rock in the upward direction makes the cavity to grow asymmetrically towards the free ground surface. Depending upon the type of rock, the depth of burial and the explosive yield, the rock may be compacted again (this is called the gas acceleration phase of the explosion) and increase its momentum. The ground surface rises as a mound. Depending upon the kinetic energy of the mound (about 15 per cent of the total energy for a depth of burst which will produce the optimum crater) and the strength properties of the rock, the mound may disintegrate or come down as a whole, producing the final apparent crater as shown in Fig. 2.

As pointed out in the introduction, the OCENER code is applicable upto the time the events described above have spherical or nearly spherical symmetry.

III. BASIC EQUATIONS IN OCENER CODE

The code employs the finite difference form of the equations of conservation of mass, momentum and energy in the spherically symmetric form. The medium is divided into spherical meshes

and a lagrangian coordinate system is used. This automatically ensures the conservation of mass as no mass is allowed to migrate from one spherical mesh to another. The equation of motion in spherical geometry is

$$\frac{1}{V}\dot{U}_R = -\left[\frac{\partial P}{\partial R} + \frac{4}{3}\frac{\partial K}{\partial R} + \frac{4K}{R} + g\right] \qquad \text{--- (1)}$$

Here V is the specific volume

$$V = \frac{1}{\rho}$$

and $\dot{U}_R$ is the acceleration in the R direction. A dot indicates the time differentiation following the particle path motion. P and K are the mean pressure and the maximum shear stress respectively, defined in terms of stress invariants, and the normal stresses, σ_R and σ_θ in R and θ directions respectively as

$$P = -(\sigma_R + 2\sigma_\theta)/3 \qquad \text{--- (2)}$$
$$= -I_1/3$$

and

$$K = (\sigma_\theta - \sigma_R)/2$$
$$= \frac{1}{2}(3 I_{2D})^{1/2}$$

Here I_1 is the first stress invariant and I_{2D} is the second deviatoric stress invariant. The equation expressing the conservation of energy is

$$\dot{E} = -P\dot{V} - \frac{2}{3} VK \left(3 \frac{\partial U_R}{\partial R} - \frac{\dot{V}}{V} \right) \qquad \text{--- (3)}$$

These two equations contain five variables V, U_R, P, K and E which are functions of R and t. The constitutive relations and the conservation of mass provide further relationships between these, e.g.

$$P = f(MU, E) \qquad \text{--- (4)}$$

$$MU = \frac{V_o}{V} - 1 \qquad \text{--- (5)}$$

$$\dot{K} = \mu \left[\frac{U_R}{R} - \frac{\partial U_R}{\partial R} \right] \qquad \text{--- (6)}$$

Here μ is the rigidity modulus, Relation (4) between the hydrostatic pressure and compressibility is dependent upon the state of the rock. The deviatoric stress (Eq 6) has to be altered depending upon the mechanical processes like ductile flow or fracturing going on in the rock. Some details of these are given in the next section.

IV. SOME COMPUTATIONAL DETAILS

The lagrangin co-ordinates are defined as

$$\rho^\circ R^{\circ 2} dR^\circ = \rho R^2 dR \qquad \text{--- (7)}$$

where the variables with superscript o denote th values at t = 0. The spherical mesh boundaries are labelled with index J; J = 1 for the centre and J = J_{max} for the outer most zone boundary. For differencing the equations given in last se_ion, the various quantities are defined in space and time as follows:

R(n, J), U(n+½, J), P(n, J-½), E(n, J-½), K(n, J-½), V(n, J-½)

Here J-½ represents the mid point of the J-1 and J mesh boundaries and n+½ has the meaning

$$\Delta t^{n+1/2} = \frac{\Delta t^{n+1} + \Delta t^{n}}{2} \qquad \text{---(8)}$$

$$t^{n+1} = t^{n} + \Delta t^{n} \qquad \text{---(9)}$$

A typical calculational cycle from time t^n to t^{n+1} proceeds as shown in the flow diagram in Fig. 3. Some of details of the various subroutines are as follows:

IV.1 SUBROUTINE EPFLOW

In this subroutine, the accelerations (Eq. 1), mesh boundaries, volume strains and K terms (Eq. 6) are calculated for all meshes at time t^{n+1} from the knowledge of the stress field (P and K) and other flow variables at time t^n. The difference form of equations used are:

(i) Acceleration

$$DU^{n+1}(J) = -\frac{1}{RRR}\left[\left\{P^{n}(J+1/2) + Q^{n}(J+1/2) - P^{n}(J-1/2) - Q^{n}(J-1/2)\right\}\right.$$
$$\left. + \frac{4}{3}\left\{K^{n}(J+1/2) + QK^{n}(J+1/2) - K^{n}(J-1/2) - QK^{n}(J-1/2)\right\}\right]\left(\frac{R^{n}(J)}{R^{*}(J)}\right)^{2}$$
$$- 4\left[\frac{K^{n}(J+1/2) + QK^{n}(J+1/2) + K^{n}(J-1/2) + QK^{n}(J-1/2)}{R^{n}(J)\left\{\frac{1}{V^{n}(J+1/2)} + \frac{1}{V^{n}(J-1/2)}\right\}}\right] \qquad \text{---(10)}$$

where

$$RRR = \frac{1}{2}\left[\frac{R^{n}_{(J+1)} - R^{n}_{(J)}}{V^{\circ}_{(J+1/2)}} + \frac{R^{n}_{(J)} - R^{n}_{(J-1)}}{V^{\circ}_{(J-1/2)}}\right]$$

Q's and QK's are the artificial viscosity terms added to the hydrostatic pressure P and deviatoric stress K respectively. These are, as is well known, for propagating steep shock fronts (see section IV. 4 below).

(ii) Velocity

$$U^{n+1/2}_{(J)} = U^{n-1/2}_{(J)} + DU^{n+1}_{(J)} \times \Delta t^{n+1/2} \qquad \text{--- (11)}$$

(iii) Mesh Boundary

$$R^{n+1}_{(J)} = R^{n}_{(J)} + U^{n+1/2}_{(J)} \times \Delta t^{n} \qquad \text{--- (12)}$$

(iv) Volume Strain

$$V^{n+1}_{(J-1/2)} = V^{\circ}_{(J-1/2)} \times \frac{R^{n+1}_{(J)^3} - R^{n+1}_{(J-1)^3}}{R^{\circ}_{(J)^3} - R^{\circ}_{(J-1)^3}} \qquad \text{--- (13)}$$

$$DV^{n+1} = V^{n+1}_{(J-1/2)} - V^{\circ}_{(J-1/2)} \qquad \text{--- (14)}$$

$$MU = \frac{V^{\circ}_{(J-1/2)}}{V^{n+1}_{(J-1/2)}} - 1 \qquad \text{--- (15)}$$

(v) K - term

$$DK^{n+1}(J-1/2) = 0.5\left[\frac{DV}{\Delta t^{n}}^{n+1} \frac{1}{V^{n+1}(J-1/2)} - 3\left\{\frac{U^{n+1}(J) - U^{n+1}(J-1)}{R^{*}(J) - R^{*}(J-1)}\right\} \times \left\{\frac{R^{n+1}(J) + R^{n+1}(J-1)}{R^{*}(J) + R^{*}(J-1)}\right\}^{2} \times \left\{\frac{V^{*}(J-1/2)}{V^{n+1}(J-1/2)}\right\}\right] \quad ---(16)$$

$$K^{n+1}(J-1/2) = K^{n}(J-1/2) + \mu\, DK^{n+1}(J-1/2)\, \Delta t^{n+1/2} \quad ---(17)$$

where

$$\mu = \frac{3}{2} k \left[\frac{1-2\nu}{1+\nu}\right],$$

$$k = -V \frac{\partial P}{\partial V}, \text{ evaluated using P-V curve (eq. 4)}$$

and ν = Poisson's ratio, which is kept fixed.

IV.2 SUBROUTINE STATE

After computation of the new hydrodynamic specific internal energy in the routine EPNEW, the subroutine STATE is called. The function of this subroutine is the determination of $P^{n+1}(J-1/2)$ depending upon the state of the rock and maximum compression seen by the zone during the shock loading. Following equations of state are used in the code.

(i) 'Iron Gas'

This is used as an approximation to the mixture of vaporised

device materials. A table containing P, E and V calculated by Godwal and Sikka (1977), using Ionisation equilibrium Saha equation of state formulation of Rouse (1971), is employed.

(ii) (SiO_2 + 1% H_2O) Gas Mixture

This is for the vaporized rock and the values of P, E and V have been taken from Butkovich (1967). This tabulated equation of state is made compatible with the Hugoniot equation of the rock. The rock mass in a given mesh is taken to be vaporised if the specific internal energy deposited in it on loading exceeds E_v, the specific internal energy for vaporisation. E_v is evaluated from the Hugoniot and the enthalpy of vaporisation (= 2800 cal/g at overburden pressure of 100 bars) for SiO_2.

(iii) Mie - Gruneisen Equation

$$P(V,E) = P_H(V) + \frac{\gamma}{V}\left[E - E_H\right] \qquad \text{---(18)}$$

$$E_H(V) = \frac{1}{2} P_H(V)\left[V_o - V\right] \qquad \text{---(19)}$$

where $P_H(V)$ and $E_H(V)$ are respectively the pressure and the specific energy at V on the Hugoniot curve. γ is the Gruneisen constant. γ = O during shock loading and also when E_{max}(the maximum specific internal energy deposited in the zone on loading) is less than E_m, the specific internal energy for melting. For the molten rock,

$$\gamma = \gamma_o \frac{E_{max} - E_m}{E_V - E_m} \qquad \text{---(20)}$$

E_m is again obtained from the Hugoniot and enthalpy of melting of the rock. The constant γ_0 is nearly equal to 1 (Cherry and Peterson, 1970).

(iv) Elastic-Plastic Region

For this region (i.e. when the rock has not been shock melted), typical loading and unloading curves are of the form shown in figure 4. If the maximum compression is upto point A, the elastic limit, the curve OA is used for both loading and unloading. For maximum loading beyond the point B, where the air filled porosity is assumed to be totally removed in the rock, the unloading is along the path BE. If the first loading is upto say C, a point between A and B, the unloading is along the path CD, which is determined by the interpolation technique described by Schatz (1973). First a slope ($\frac{dP}{dMU}$) is defined as

$$\left(\frac{dP}{dMU}\right)^{n+1/2} = \left(\frac{dP}{dMU}\right)_L + \frac{MU^{max}}{MU_2}\left[\left(\frac{dP}{dMU}\right)_U - \left(\frac{dP}{dMU}\right)_L\right] \qquad \text{--- (21)}$$

where the slopes with subscripts L and U are slopes of the loading and unloading P - MU curves, evaluated at the old pressure. The new pressure is then given by

$$P^{n+1}(J-1/2) = P^{n}(J-1/2) + \left(\frac{dP}{dMU}\right)^{n+1/2}\left[\frac{V^{s}(J-1/2)\{V^{n}(J-1/2) - V^{n+1}(J-1/2)\}}{V^{n+1}(J-1/2)\, V^{n}(J-1/2)}\right] \qquad \text{-- (22)}$$

To monitor the type and state of the rock material in each zone $(J-\frac{1}{2})$, a two digit parameter $IT(J-\frac{1}{2})$, is used. The least

significant digit of this represents the type of rock and can assume integral values from 1 to 9 (9 different rocks). The second characterises the state of the rock according to the following scheme.

State of Rock	IT(J-½)
Elastic-Plastic and shock loading	11 - 19
Elastic-Plastic and shock unloading	21 - 29
Molten rock loading	31 - 39
Molten rock unloading	41 - 49
Vaporized rock	51 - 59
Iron gas	61

IV.3 SUBROUTINE FAILURE

In this subroutine the value of K, evaluated from equation (17), is adjusted for the type of deformation undergone by the material in the mesh. This need for adjustment arises because the rock material, when it fails (ductile or brittle failure), can no longer sustain the original deviatoric stress. In the code, the following relaxation schemes for K^{n+1} have been provided.

(i) Vaporised or melted rock

$$If \quad E^{n+1} > E_m$$

$$K_A^{n+1} = 0$$

Here K_A^{n+1} denotes the adjusted value of K^{n+1}.

(ii) Plastic and Ductile Flow

$$If \quad P^{n+1} + \frac{1}{3} K^{n+1} \geq P^{BD}$$

$$and \quad |K^{n+1}| \geq K^{max}$$

$$K_A^{n+1} = \frac{E_m - E^{n+1}}{E_m} K^{max} \times \text{sign of } K^{n+1}$$

P^{BD}, the brittle ductile transition point and K^{max}, the maximum deviatoric stress allowed by the failure curve for a rock are defined in Fig. 5.

(iii) Brittle Fracture

$$If \quad P^{n+1} + \frac{1}{3} K^{n+1} < P^{BD}$$

and if K^{n+1} is greater than the value of K allowed by the failure curve, then brittle crack is allowed to be formed. The failure curve for each rock type is read in the form of a table containing $K_{failure}$ and $\bar{P}$ ($=P+K_{failure}/3$) values. This data is either generated from the experimental triaxial compression and tension tests or evaluated from the measurement of the unconfined compressive strength and the average normalised strength curves for rocks given by Ohnaka (1973) and Gupta and Sikka (1978). Once the crack is initiated, the adjustment of K is done as follows:

$$K_A^{n+1} = \frac{E_m - E^{n+1}}{E_m} K_{lim} \times \text{Sign of } K^{n+1}$$

where $$K_{lim} = |K^{n+1}| \left[1 - \frac{C_V C_R}{4\{R^{n+1}(J) - R^{n+1}(J-1)\}} \Delta t^n \right] \leq K^{max}$$

$$C_V = 1.14 \sqrt{\frac{\mu}{\rho_o \left(3 + \frac{\mu}{k}\right)}}$$

$$C_L^{n+1} = C_L^n + C_V \Delta t^n$$

$$C_R = \frac{C_L^{n+1}}{4\{R^{n+1}(J) - R^{n+1}(J-1)\}} \leq 1$$

This relaxation process is assumed to operate until K_A^{n+1} becomes half the limiting shear stress for the fractured rock. Then material is assumed to have cracked (a parameter $N_{crack}(J-\frac{1}{2})$ is incremented by one). Henceforth, K^{n+1} is compared with K allowed by the failure curve for the cracked material, for entering into this part of the subroutine. This is taken to be straight line from the origin to P^{BD}.

Also, if during this cracking process, any principal stress is found to be tensile, K_{lim} is immediately set equal to zero and then crack number is increased by one.

IV.4 ARTIFICIAL VISCOSITY TERM

To cater to the propagation of steep shock fronts by equation of motion, artificial viscosity terms (both quadratic and linear) are added to P and K in the equation of motion (see section IV.1.i). This term for P is

$$Q^{n+1}_{(J+1/2)} = C_1 \rho (DU)^2 + C_2 C_0 \rho |DU|$$

where $$DU = U^{n+1}_{(J+1)} - U^{n+1}_{(J)}$$

$$= 0 \quad \text{if} \quad DU > 0$$

and $$C_0 = \sqrt{\frac{\frac{\partial P}{\partial \mu U} + \frac{4}{3}\mu}{\rho_0}}$$

For the K term, the artificial viscosity term is of the form

$$QK^{n+1}_{(J+1/2)} = C_3 C_0 \rho \left\{ R^{n+1}_{(J+1)} - R^{n+1}_{(J)} \right\} DK^{n+1}_{(J+1/2)}$$

$$C_3 = C_4 \cdot 2\mu \Big/ \left(\frac{\partial P}{\partial \mu U}\right)$$

C_1, C_2, C_4 are constants having values of order 2.0, 0.2 and 0.075 respectively.

IV.5 Δt CALCULATION

The quantity

$$WR = \frac{\Delta t^n \left\{ 16 C_1^2 (DU^{n+1/2})^2 + (1 + 4 C_2^2) C_0^2 \right\}^{1/2}}{R^{n+1}_{(J)} - R^{n+1}_{(J-1)}}$$

is calculated for each mesh. The time step is then determined using the maximum value of W_R over all meshes as below:

$$\Delta t^{n+1} = 0.5 \times \Delta t^{n} \qquad \text{for} \quad W_{R\,max} > 0.3$$

$$= \Delta t^{n} \qquad 0.1 \leqslant W_{R\,max} \leqslant 0.3$$

$$= 2.0 \times \Delta t^{n} \qquad W_{R\,max} < 0.1$$

IV.6 BOUNDARY CONDITIONS

For a cratering type explosion, when the shock wave meets the ground surface, free surface boundary conditions are used.

IV.7 INITIAL CONDITIONS

In the code, a calculation can be started by the following models:

(i) 'Iron-Gas' Model

In this model, the energy of the device is released into the volume of the firing chamber, conventionally taken to be $1m^3$, and the initial magnitude of the shock wave amplitude evaluated from the specific internal energy and equation of state of the vaporised device components, assumed to be 'iron gas' or 'SiO_2 gas' as described in STATE.

(ii) Bubble Model

In this model, the energy is given to the vaporized rock cavity of radius

$$R_V = 2.557 \left(\frac{W}{\rho_{EP}} \right)^{1/3}$$

for a silicate rock. W is the yield of the nuclear explosive in kilotons and ρ_{EP} is the density of the rock surrounding the device. This expression for R_v is based on the assumption that 70 tons of rock is shock vaporized per kiloton of energy released by the nuclear device (But'kovich, 1967).

IV. 8 REZONING

The code has provision for regrouping of the meshes at the end of each cycle or after n cycles. This is useful, since the value of Δt is determined by (see section IV. 5) the thickness of the narrowest mesh and if it is too small, it would increase the total computational time.

If the thickness of the narrowest mesh becomes less than two-thirds of its value at t = O, this is combined with one of its adjacent meshes. Two meshes of different rock types are never combined. When two meshes are regrouped, the state of the inner-most mesh is attributed to the new mesh thus formed. The volume and mass of the new mesh are assumed to be equal to the sum of the volumes and masses of the two regrouped meshes. The internal energy, the pressure and the deviatoric stress of the new mesh are determined by summing the mass-weighted quantities of the regrouped meshes. The mesh index J remains unchanged for all the zones occuring before the new mesh and the index of the following meshes is reduced by one.

IV.9 SIMULATION OF OVERBURDEN PRESSURE

The code provides the following options for calculating the effect of overburden on shock propagation: (1) in free-field approximation when gravity effects are ignored, (2) in horizontal direction and (3) in vertical direction.

In case of horizontal wave propagation, each mesh is subjected to a constant pressure $\rho g h$ (h = depth of emplacement) exerted by the rock overburden above the detonation point. The starting specific volume of the meshes at this pressure is obtained by using the P-MU loading table for the rock.

For the wave propagation in the vertical direction, each mesh is under different overburden pressure, depending on its distance from the surface ground zero. This pressure and the resulting specific volume and internal energy for each mesh and the new mesh boundaries are determined using the following equations.

$$P^{\circ}(J-\tfrac{1}{2}) = 0.5\, g\, \rho^{\circ}(J-\tfrac{1}{2})\left\{ R^{\circ}(J) - R^{\circ}(J-1)\right\}$$

$$+ 0.5\, g\, \rho^{\circ}(J_{max}-\tfrac{1}{2})\left\{ R^{\circ}(J_{max}) - R^{\circ}(J_{max}-1)\right\}$$

$$+ \sum_{I=J+1}^{J_{max}-1} g\, \rho^{\circ}(I-\tfrac{1}{2})\left\{ R^{\circ}(I) - R^{\circ}(I-1)\right\} \qquad \text{for } J_0 < J < J_{max}$$

The specific volume $V(J-\frac{1}{2})$ is obtained using the P-MU table

$$V(J-1/2) = \frac{1}{\rho^{\circ}(J-1/2)} \frac{1}{MU(J-1/2)+1} \qquad J_e < J < J_{max}$$

$$HMAS(J-1/2) = \frac{4\pi}{3}\left[R(J)^3 - R(J-1)^3\right] \rho^{\circ}(J-1/2) \qquad J_e < J < J_{max}$$

$$E^{\circ}(J-1/2) = 0.5 \times P^{\circ}(J-1/2) \times MU(J-1/2) \qquad J_e < J < J_{max}$$

$$R(J) = \left[R^{\circ}(J-1)^3 + \frac{3}{4\pi}\left\{HMAS(J-1/2)\, V(J-1/2)\right\}\right]^{1/3} \qquad J_e < J < J_{max}$$

V. SOME TYPICAL OUTPUTS

Some of the typical outputs of this program are the following:

1) the amount of shock-vaporised rock;

2) the amount of shock-melted rock;

3) the radius of the cavity and the pressure inside it at any given time;

4) profiles of shock position versus time, peak stress (both hydrostatic and deviatoric) versus radius, particle velocity versus radius etc;

5) spall velocities of the mesh points as the reflected tensile wave from the surface travels towards the growing cavity; and

6) the extent and type of rock failure (ductile or fracture).

VI. SAMPLE CALCULATIONS

To test the code, two sample calculations were run. These were (i) a 5 kt detonation in Hardhat granite and (ii) a 3 kt explosion at a depth of 52 m in a layered rhyolite medium (ρ^o for the layer extending from the surface down to 20 m above the shot point = 1.98 g/cm^3 and ρ^o = 2.51 g/cm^3 for the rest of the medium) similar to that for the Cabriolet event in USA. Some of the values for the material properties of these rocks were taken from the papers of Cherry(1967) and Cherry and Petersen (1970) and the rest generated from a program similar to PMUGEN (Butkovich, 1973). These are given in table 1.

Table 1. Material Properties Used in Test Calculations

	Granite	Rhyolite(deep)	Rhyolite(top)
Initial density (g/cc)	2.67	2.517	1.98
Water Content (wt %)	0.0	0.0	0.0
Poisson's ratio	0.28	0.20	0.20
Initial Bulk Modulus (Mbar)	0.361	0.104	0.014
Brittle-ductile point (Mbar)	0.005	0.0015	0.0015
Pressure-volume relation	see Teller et al (1968)	see Cherry (1967)	see Cherry (1967)
Strength curve	wet. case (Fig. 22 of Cherry and Petersen, 1970)	From PMUGEN	From PMUGEN

The 'Bubble' model was used to initiate the calculations. For granite, we compared the peak pressure vs scaled radius as computed by our code, with that given by Cherry and Petersen (1970). This is shown in fig. 6. For the rhyolite medium, a comparison of the mound velocity profile, when the shock wave reaches the ground surface, with that given by Cherry (1967) is presented in Fig. 7. In view of the fact that some of the values for the material properties used by us may not be the same as those used by Cherry (1967) and Cherry and Petersen (1970), the agreement between our curves and theirs is good.

REFERENCES

1. Butkovich T.R. (1967), Lawrence Radiation Laboratory, Livermore, Rept. UCRL-14729.
2. Butkovich T.R. (1973), Lawrence Livermore Laboratory, Livermore, Rept. UCRL-51447.
3. Cameron I.G. and Scorgie G.C. (1970), Proc. Tech. Committee on Peaceful Nuclear Explosions I, IAEA, Vienna, 331.
4. Cherry J.T. (1967), Int. J. Rock Mech. Min. Sci. 4, 1.
5. Cherry J.T. and Peterson F.L. (1970), Proc. Tech. Committee on Peaceful Nucl. Explosions I, IAEA, Vienna, 241.
6. Chidambaram R. and Ramanna R. (1975), Proc. Tech. Committee on Peaceful Nucl. Explosions IV, IAEA, Vienna, 421.
7. Godwal B.K. and Sikka S.K. (1977), Pramana 8, 217-222.
8. Gupta S.C. and Sikka S.K. (1978), Bhabha Atomic Research Centre Rept. BARC-968.
9. Maury J. (1970), Lawrence Livermore Laboratory, Rept. UCRL-Trans-10617-9.
10. Ohnaka M. (1973), J. Phys. Earth, 21, 125.
11. Schatz J.F. (1973), Lawrence Livermore Laboratory, Livermore, Rept. UCRL-51352.
12. Schatz J.F. (1974), Lawrence Livermore Laboratory, Livermore, Rept. UCRL-51689.
13. Rouse C.A. (1971), "Progress in High Temp. Physics and Chemistry" (Pragamon Press: Oxford) Vol. 4, p.139.

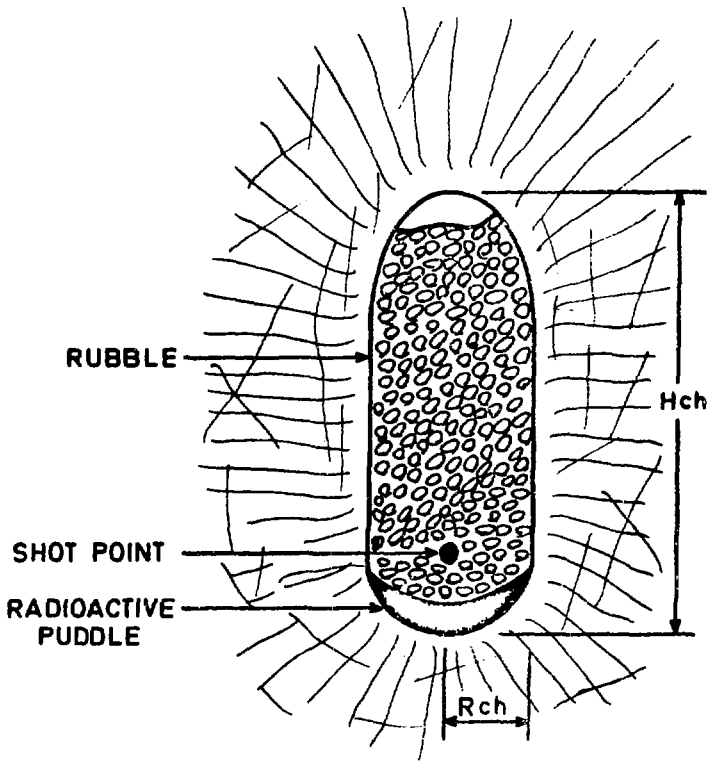

Fig. 1. Cross section of a chimney produced in hard rock for a deeply burried nuclear explosion.

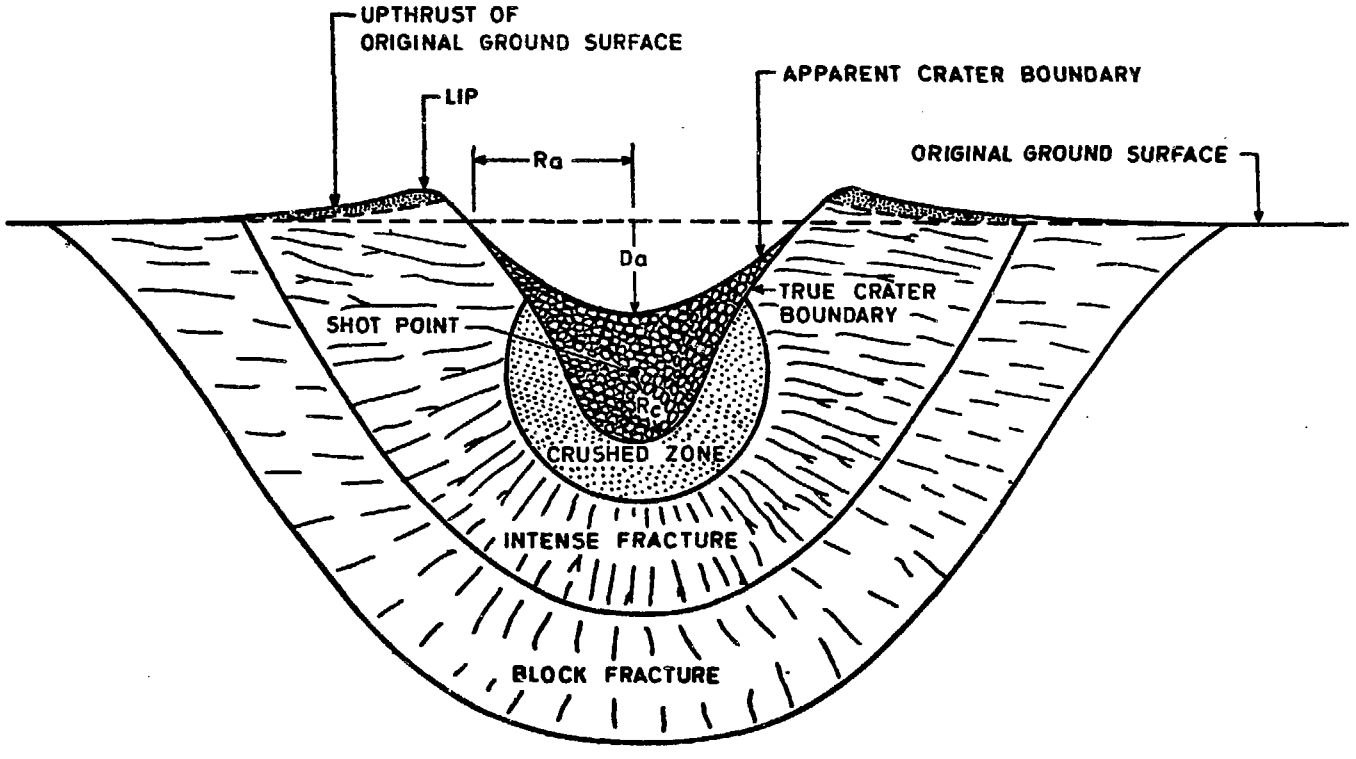

Fig. 2. Cross section of a crater produced by a nuclear explosion.

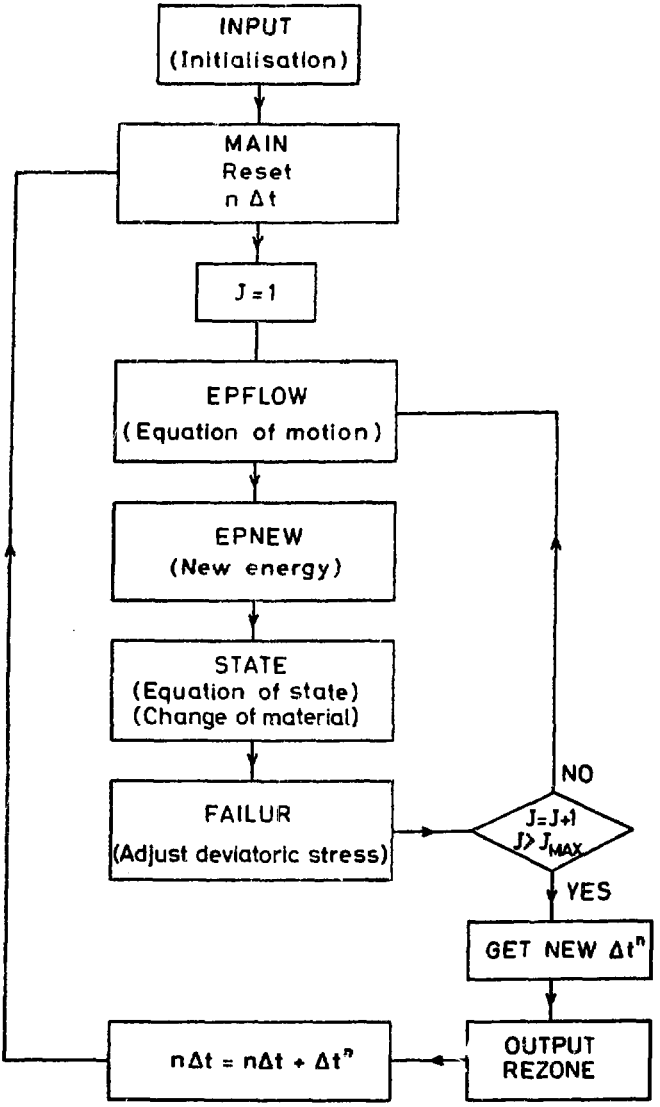

Fig. 3. Schematic flow diagram for the "OCENER" code

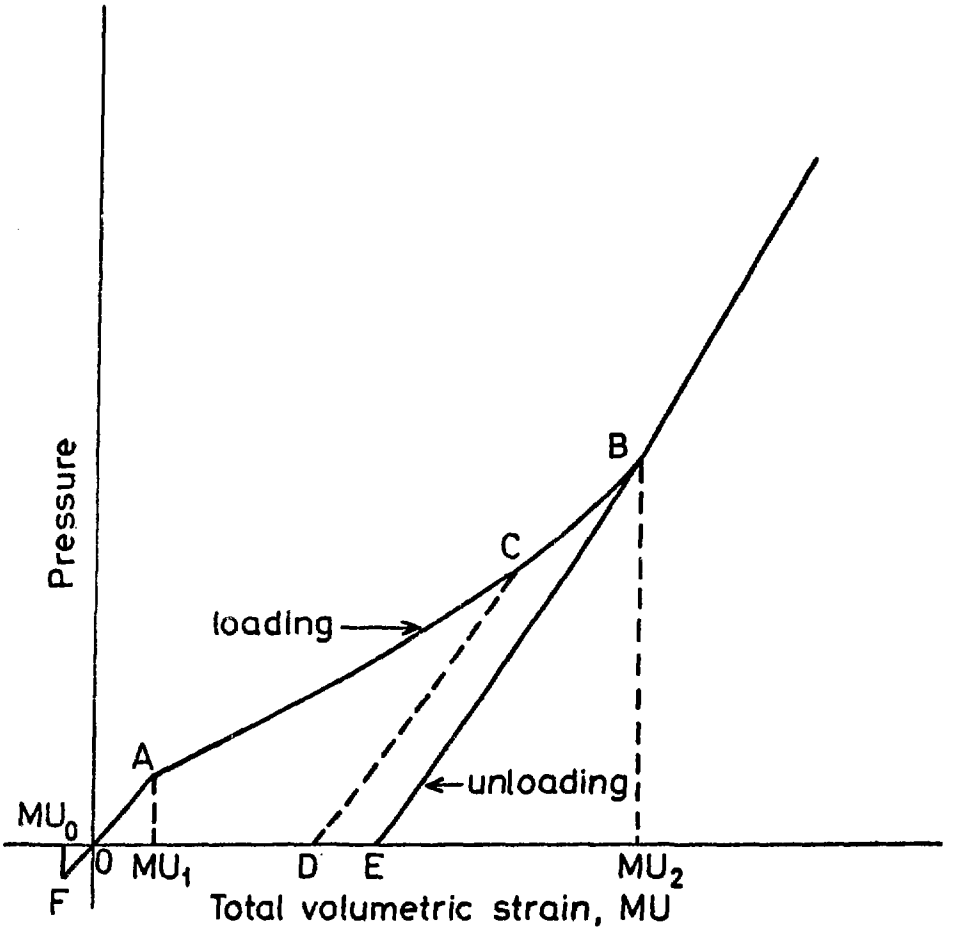

Fig. 4. Typical loading and unloading curve in P-MU plane. MU_0 is the bulking strain. MU_1 is the strain upto which material is to be treated elastically and at MU_2 the air filled porosity is completly removed.

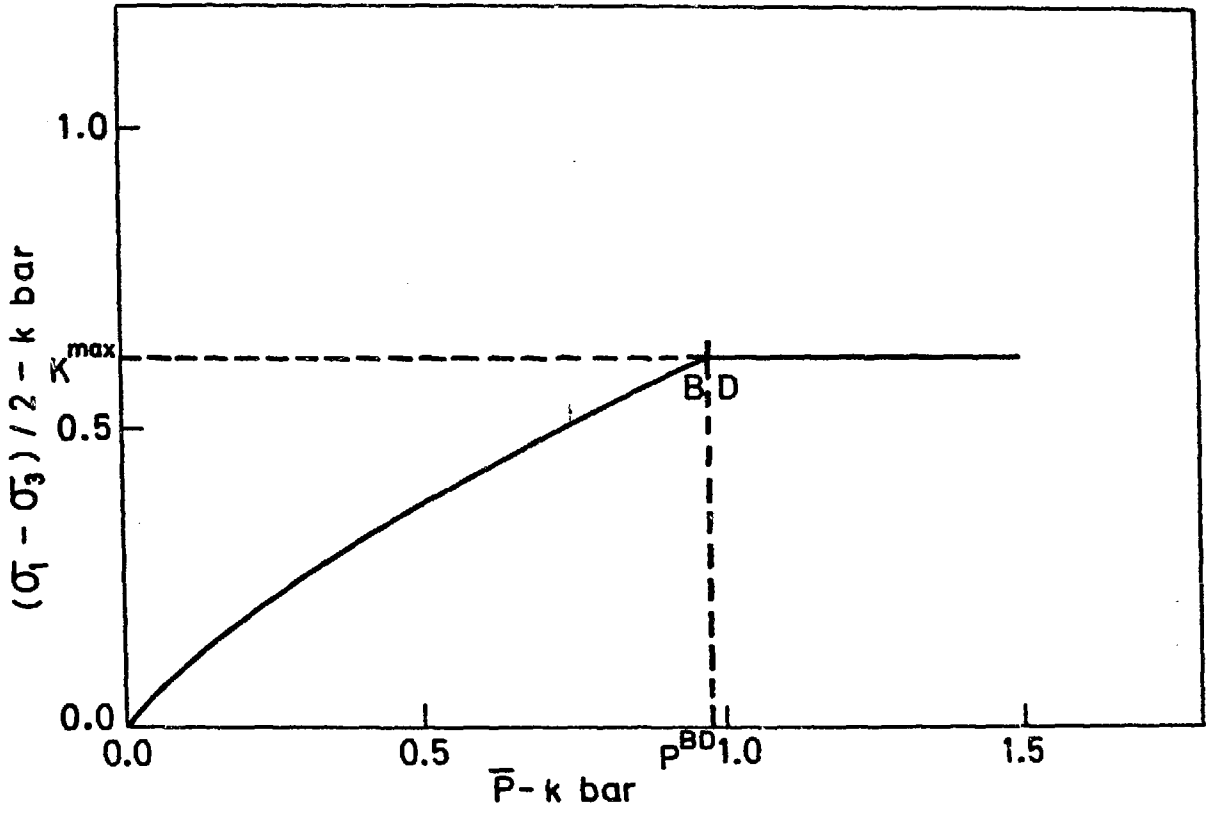

Fig. 5. A typical shear strength curve

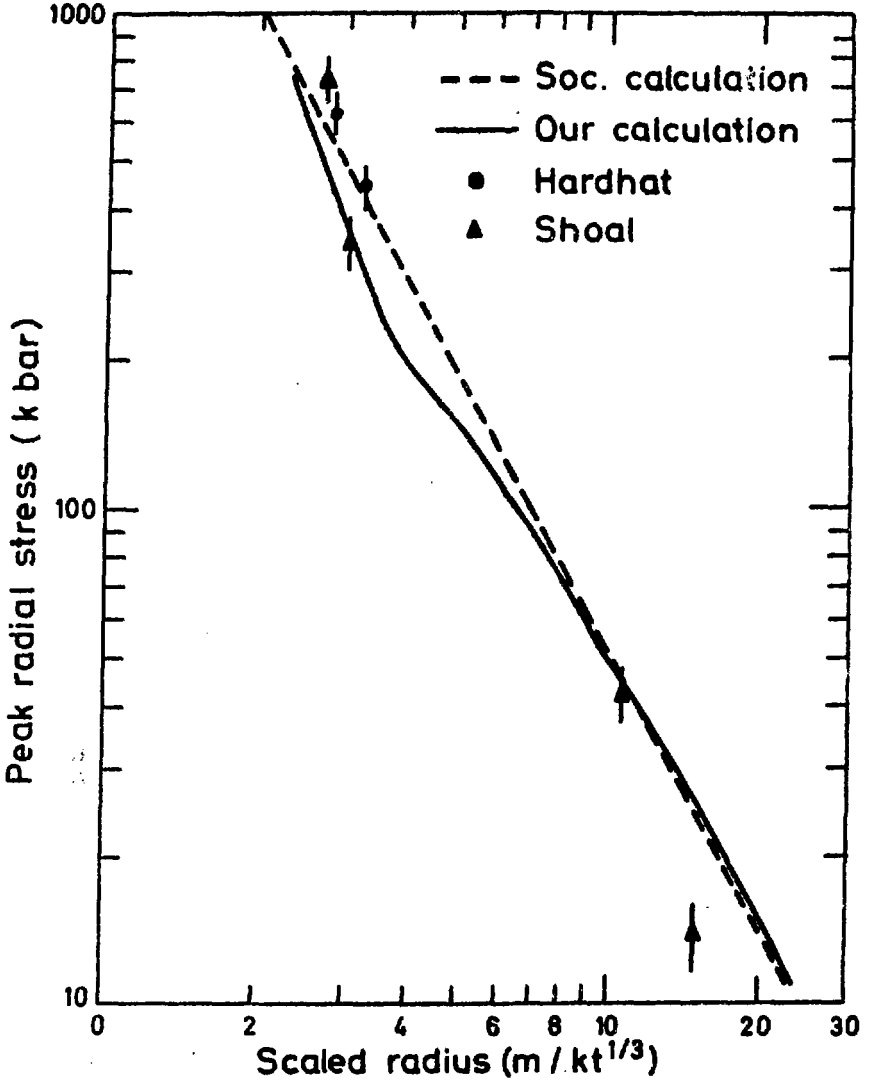

Fig. 6 Peak radial stress profile in granite

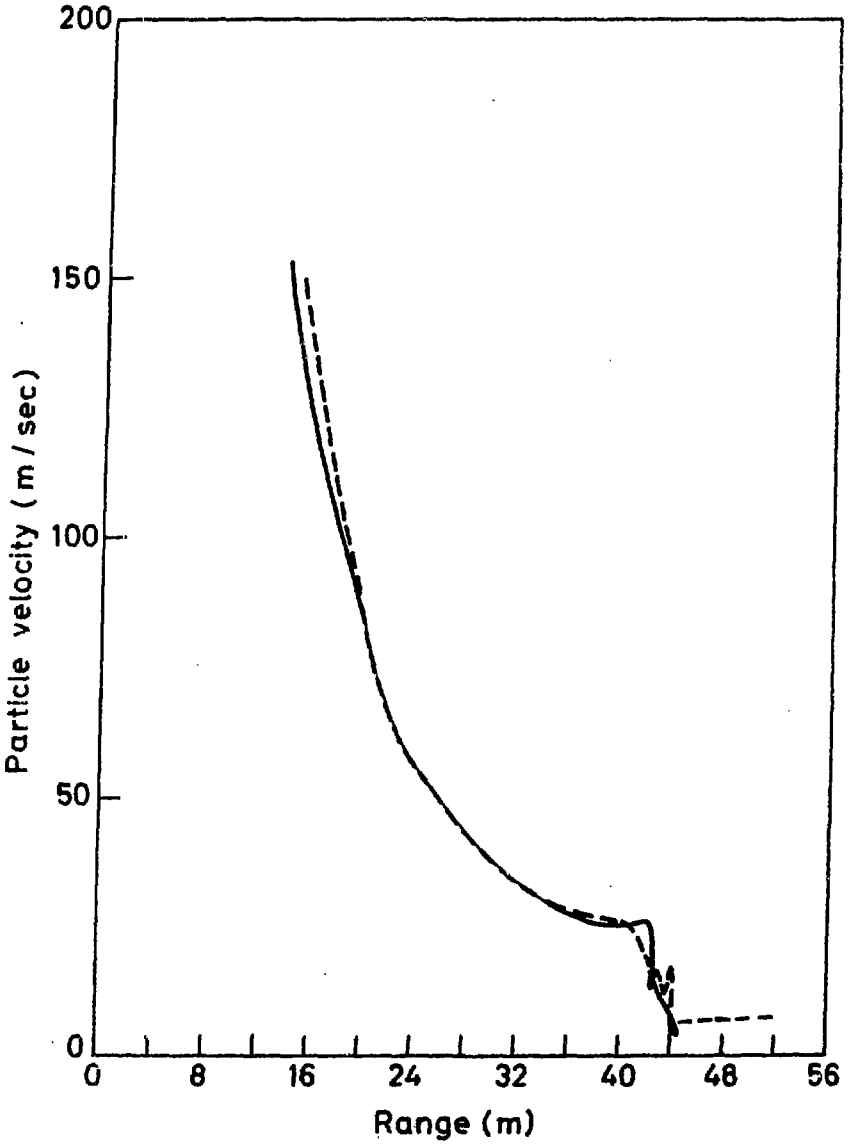

Fig. 7. Particle velocity profiles at the time when the shock reaches surface ground zero. ——our calculation,---Cherry's (1967) calculation.

APPENDIX - DATA INPUT

1. Title Card — FORMAT (12A6)

Columns	
1-72	Title consisting of any desired Hollereth information to identify the problem.

2. Explosion parameter cards — FORMAT (2F 10.4, 2I5)

(a) Columns

1-10	W, the yield of device in kilotons.
11-20	DEPTH, the depth of burial of the device in meters
21-25	IG, the type of calculation indicator IF IG = O, the calculation is done for the case of free field motion where the gravity effects are ignored. IF IG = 1, the calculation is done for horizontal direction; the effects of gravity are included. IF IG = 2, the calculation is done for vertical direction, the density variation due to the overburden pressure is accounted for.
26-30	IR equals the number of rock types used in the calculation. The maximum value of IR allowed is 9. This is limited by the memory of the BESM-6 computer.

(b) FORMAT (F 10.4, E12.5)

Columns	
1-10	RC, the radius in meters of initial spherical chamber. For 'Bubble' model, it is calculated using equation (23) in the text.
11-22	VPMASS, the vaporised mass in the cavity chamber RC. For iron gas model, it is the mass of the device; for 'Bubble' model, VPMASS = W x 70 x 10^6 gms.

3. Material Properties cards

The material properties for all IR number of rocks are given in these cards. The number of cards required for each property depends on the value of IR.

FORMAT (6E12.5)

(a) DENSITY (I), I = 1, IR	Initial density (g/cm^3)
(b) EV (I), I = 1, IR	Specific internal energy for vaporization (10^{12} ergs/g)
(c) EM(I), I = 1, IR	Specific internal energy for melting (10^{12} ergs/g)
(d) XKS(I), I = 1, IR	Initial bulk modulus (Mbar)
(e) XMUS(I), I = 1, IR	Initial rigidity modulus (Mbar)
(f) XNU(I), I = 1, IR	Poisson's ratio

(g) XMLAST(I), I = 1, IR — MU_1

(h) XMU_2(I), I = 1, IR — MU_2 (see Fig. 4)

(i) XMUO(I), I = 1, IR — MU_O

(j) BD(I), I = 1, IR — Brittle-ductile transition point(Mbar)

(k) BDK(I), I = 1, IR — K^{max}(Mbar)

4. Loading and unloading P-MU and strength tables

(a) First card — FORMAT (2I5)

Columns

1-5 — MPMU number of data points in each of the P-MU tables

6-10 — MKP number of data points in each of K-P tables.

(Both MPMU and MKP have same values for all the IR sets).

(b) Second Card set 1 (I = 1, for the first set; I = 2, for second set and so on).

FORMAT (8F 10.4)

P(I, J), J = 1, MPMU — Pressure values (Mbar)

MUL(I, J), J = 1, MPMU — Corresponding MU Loading values

MUU(I, J), J = 1, MPMU — Corresponding MUunloading values

PBAR(I, J), J = 1, MKP — $\bar{P}$ values

XK(I, J), J = 1, MKP — K values

(sets 1 to IR will occur in succession)

5. Set of cards for dividing the medium into spherical meshes

Suppose the calculations are to be done upto a radius of D_{max}.

One may have to divide this into different zones, either containing different rock types or, in any given zone (same rock type), one may like to have meshes of different widths. As an example, we give the cards for the following division of material around the detonation point.

Range (m)	number of meshes	density(gm/cm^3)	Rock type
$O - D_1$	n_1	$DENSITY_1$	L_1
$D_1 - D_2$	n_2	$DENSITY_2$	L_2
$D_2 - D_3$	n_3	$DENSITY_3$	L_3
-----	--	----	--
$D_{n-1} - D_{max}$	n_n	$DENSITY_n$	L_n

(a) First Card FORMAT(I5)

Column

1-5 N_{max}, total number of meshes

(b) Second Card FORMAT (6(I1, I2, F9.4)

(Divides the rock medium surrounding the detonation point into meshes of specified width).

Columns

1 $K_1 = O$

2-3 $N_1 = n_1 - 1$

4-12 $D_1 = O.O$

13 $K_2 = 2$

14-15 $N_2 = n_2 - 1$

16-24 D_2

25	$K_3 = 2$	
26-27	$N_3 = n_3$-1	
28-36	D_3	
	till $D_n = D_{max}$	
	then $K_{n+1} = 3$	which indicates completion of meshing.

(c) Third card FORMAT (6(I1, I2, E 9.4)

(specifies the densities of each of the meshes).

Columns		
1	$K_1 = 1$	
2-3	$N_1 = n_1$	sets $\rho(I)$ = DENSITY$_1$ for I = 1 to N_1
4-12	DENSITY$_1$	
13	$K_2 = 1$	
14-15	$N_2 = n_2$	sets $\rho(I)$ = DENSITY$_2$ for I = N_1+1 to N_1+N_2
16-24	DENSITY$_2$	
	till $N_1+N_2+N_3 \ldots N_n = N_{max}$	
	then $K_{n+1} = 3$	Termination index

(d) Fourth card FORMAT (6(I1, I2, I9))

(indicates the rock type in each mesh)

Columns		
1	$K_1 = 1$	
2-3	$N_1 = n_1$	sets IT(I) = L_1 for I = 1 to N_1
4-12	L_1	
13	$K_2 = 1$	

14-15 $N_2 = n_2$ sets $IT(I) = L_2$ for $I = N_1+1$ to N_2+1

16-24 L_2

till $N_1+N_2+N_3 + \ldots + N_n = N_{max}$

$K_{n+1} = 3$ Termination index